

## Article

# Land Consumption Mapping with Convolutional Neural Network: Case Study in Italy

Giulia Cecili <sup>1,\*</sup>, Paolo De Fioravante <sup>2</sup>, Luca Congedo <sup>2</sup>, Marco Marchetti <sup>1</sup> and Michele Munafò <sup>2</sup><sup>1</sup> Department of Biosciences and Territory, University of Molise, C/da Fonte Lappone, 86090 Pesche, Italy<sup>2</sup> Italian Institute for Environmental Protection and Research (ISPRA), Via Vitaliano Brancati 48, 00144 Rome, Italy

\* Correspondence: g.cecili@studenti.unimol.it

**Abstract:** In recent years, deep learning (DL) algorithms have been widely integrated for remote sensing image classification, but fewer studies have applied it for land consumption (LC). LC is the main factor in land transformation dynamics and it is the first cause of natural habitat loss; therefore, monitoring this phenomenon is extremely important for establishing effective policies and sustainable planning. This paper aims to test a DL algorithm on high-resolution aerial images to verify its applicability to land consumption monitoring. For this purpose, we applied a convolutional neural networks (CNNs) architecture called ResNet50 on a reference dataset of six high-spatial-resolution aerial images for the automatic production of thematic maps with the aim of improving accuracy and reducing costs and time compared with traditional techniques. The comparison with the National Land Consumption Map (LCM) of ISPRA suggests that although deep learning techniques are not widely exploited to map consumed land and to monitor land consumption, it might be a valuable support for monitoring and reporting data on highly dynamic peri-urban areas, especially in view of the rapid evolution of these techniques.

**Keywords:** deep learning; convolutional neural networks; land consumption mapping; land cover; remote sensing; semantic segmentation



**Citation:** Cecili, G.; De Fioravante, P.; Congedo, L.; Marchetti, M.; Munafò, M. Land Consumption Mapping with Convolutional Neural Network: Case Study in Italy. *Land* **2022**, *11*, 1919. <https://doi.org/10.3390/land11111919>

Academic Editor: Rohan Bennett

Received: 29 September 2022

Accepted: 24 October 2022

Published: 28 October 2022

**Publisher's Note:** MDPI stays neutral with regard to jurisdictional claims in published maps and institutional affiliations.



**Copyright:** © 2022 by the authors. Licensee MDPI, Basel, Switzerland. This article is an open access article distributed under the terms and conditions of the Creative Commons Attribution (CC BY) license (<https://creativecommons.org/licenses/by/4.0/>).

## 1. Introduction

### 1.1. Background

Soil is one of the most complex and extremely fragile natural resources which provides fundamental ecosystem services for human wellbeing, society, and the environment, such as food production, biomass, raw materials, climate regulation, carbon storage, etc. [1–5]. Soil health is essential to meet the needs of current and future generations; therefore, it is a central topic in sustainable development strategies [2].

In recent years, rapid urbanization, industrialization, and infrastructure development are among the global trends which determined many land use and land cover changes [6]. Landscape changes are shaping society, the biosphere, and endangering soil health: about three-quarters of the Earth's surface has undergone anthropic pressures during the last centuries [7], becoming the most widespread cause of arable land loss, habitat destruction, and climate changes [2,8].

Land consumption (LC) is the land transformation process related to the construction of new buildings, the expansion of cities, the infrastructure of the territory, and other soil sealing interventions [2,9,10]. Land consumption is defined as the loss of agricultural, natural, and semi-natural areas due to the new artificial cover [2]. Due to LC, the soil loses its ability to provide ecosystem services and sustain biodiversity; it negatively affects our wellbeing and quality of our lives [2,11].

Land consumption monitoring represents a fundamental activity for effective policies and sustainable planning [6]. Remote sensing has proved over the years to be an extremely

powerful tool for land monitoring [7,8,12–14]. In this context, land use (LU) and land cover (LC) classifications play a crucial role in monitoring environment dynamics, studying phenomena such as deforestation, land degradation, or land consumption, and supporting applications such as sustainable spatial planning and resource management policies [15,16].

In detail, the use of remote sensing has contributed to the creation of several cartographic products related to land consumption at the national and European levels. Among European products, there is the imperviousness degree layer (IMD), which is one of the four strata (imperviousness, forest, grassland, water, and wetness) belonging to the Copernicus Pan-European High-Resolution Layers (HRLs). The imperviousness product is a raster map with a spatial resolution of 10 m and with an update frequency of three years, which represents the degree of imperviousness of each pixel ranging from 0 to 100 (<https://land.copernicus.eu/pan-european/high-resolution-layers>, accessed on 29 April 2022). At the national level, ISPRA has been monitoring land consumption in Italy since 2006 through the publication and the annual update of the National Land Consumption Map (LCM) [2,6,17]. The final product is a 10 m resolution raster for the whole national Italian territory [2], with an overall accuracy of 99.7% [18].

This document presents a first attempt to propose a methodology to automate the monitoring of land consumption, exploiting the innovative technologies of deep learning for the management of big data [19] with a marginal intervention of the photointerpreter. With the development of new technologies, Earth observation environmental data are growing rapidly in complexity, size, and resolution [20], offering an unprecedented monitoring possibility. This information is called “big geospatial data” [21] and it is still underused. The underuse of this technology causes a loss of time and potential in decision-making processes [22].

Recently, the use of the deep learning (DL) has rapidly grown in the data analysis field. The application of this technology was made possible by two main factors: the increased availability of data and the increased computational capability [23]. Due to the progress made by the scientific community, DL has been successfully applied to a variety of fields [24,25] and is now considered a state-of-the-art technology in many areas. Remote sensing image classification is certainly one of these areas [26,27].

DL is a subcategory of machine learning (ML), which corresponds to the concept of artificial neural networks (ANNs). By learning from a set of ground truth data, these algorithms can perform specific tasks without explicit instructions and offer high predictive accuracy even when complex non-linear relationships exist. Hierarchical learning is followed by ANNs, which are made of multiple layers of artificial neurons. In order to produce the outputs, the network combines the inputs and modifies them according to weights, biases, and activation functions [28,29].

A family of DL algorithms known as convolutional neural networks (CNNs) has recently achieved significant results in computer vision [30]. It is particularly effective at detecting lines, angles, curves, etc., in the input image. The convolution operator is what makes them so effective for image classification [31].

CNNs have been used for land cover classification in remote sensing data; as a matter of fact, some studies investigated wetlands [32,33], while others investigated urban areas [34–37]. On the other hand, several studies have primarily focused on natural classes [38,39] or agricultural production areas [40].

These algorithms are nowadays the most popular in remote sensing due to their exceptional performance [29]. Indeed, if compared with other traditional pixel-wise models such as random forest (RF) or support vector machine (SVM), the CNNs have the following advantages: the ability to work directly with raw images, the reduction in input noise, the low overfitting tendency, and the ability to recognize elements even in rotated or distorted images (typical in remote sensing) [23,31,41].

### 1.2. Operational Requirements

Using traditional methods for cartographic production and updating involves low update frequencies, which compromises the possibility to use them in applications that require rapid and timely intervention [42]. The main LC/LU Copernicus data are updated every 3 or 6 years, while the LCM is the only data available for consumed land mapping at the national scale that has an annual update frequency. LCM updating is extremely time consuming since it requires manual inspection of the entire national territory and photointerpretation of the new land consumption. To this end, ISPRA has launched studies to make this activity less burdensome and less time consuming. Currently, some support products for photointerpretation have been introduced, called “masks of potential changes” [1,17] that narrow the area of investigation (it can be limited to 2.4% of the national territory) and significantly reduce the photointerpretation effort. However, there is still a need for tools that simplify data updating while maintaining high reliability, especially in peri-urban areas, where the greatest density of change occurs.

### 1.3. Objective

The study aims to show the high potential of CNNs in consumed land mapping as a preliminary step for using these tools in land consumption monitoring. In detail, the activity seeks for the first time to develop tools based on DL techniques that can be integrated into the updating process of the LCM carried out by ISPRA for the Italian territory. As there are few studies on the use of deep learning to assess land consumption, the results of this research offer the opportunity to explore the potential of deep learning to analyze this negative human impact on the landscape.

The objectives of the study are summarized as follows:

1. Testing of the DL in consumed land mapping;
2. Automatic production of thematic maps with the aim of improving accuracy and reducing costs and time compared with traditional techniques;
3. Demonstration of the strategic importance of artificial intelligence for the future of environmental monitoring, with particular reference to land consumption mapping.

The study shows an application of a CNN architecture called ResNet50 to detect consumed land. The training and validation of the model was carried out on a first study area located in the municipality of Rome, which was chosen in order to present a mixed composition in terms of natural and artificial land cover classes. The classification methodology was tested with reference to three different configurations of parameters (called “scenarios”). The most suitable scenario has been applied to new test areas located in the Italian region of Tuscany.

## 2. Materials and Methods

### 2.1. Study Area

The study area includes six sites located among the provinces of Florence, Siena, and Arezzo, in the Italian region of Tuscany (Figure 1). The six areas have a total area of 67.6 km<sup>2</sup> and are located at a latitude between 43°29′50.19″ N and 43°36′4.24″ N and a longitude between 11°19′46.39″ E and 11°32′35.33″ E. For the training and validation of the deep learning model, reference was made to an area of 5.7 km<sup>2</sup> located in the municipality of Rome (Figure 2).

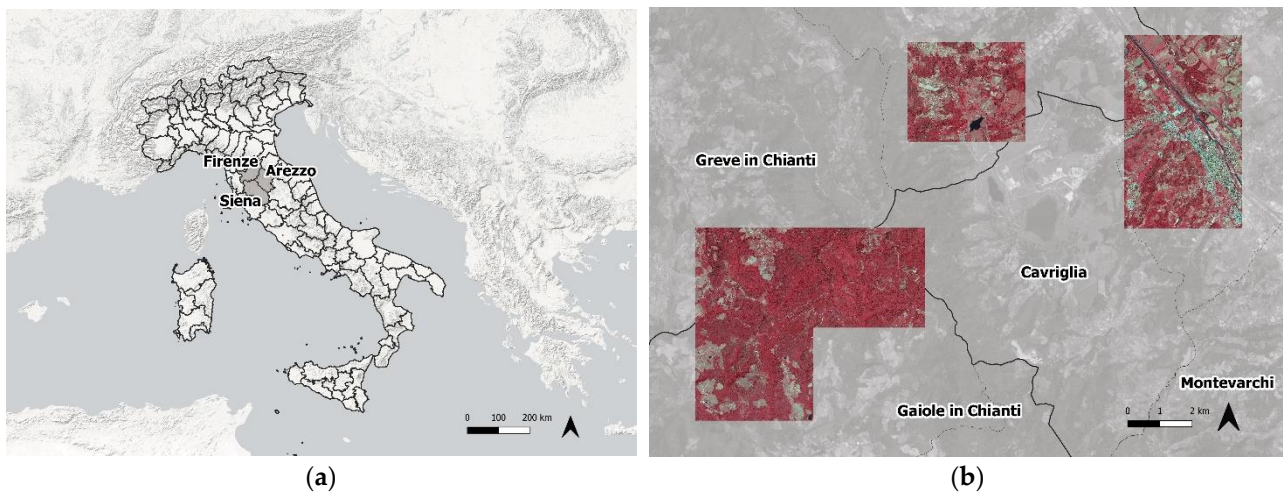


**Figure 1.** (a) Location of the study areas in Italy; (b) study areas.



**Figure 2.** (a) Training area; (b) validation area.

## 2.2. Overview

The proposed methodology applied the deep learning algorithms on orthophoto images to verify the feasibility of creating land cover classification, with particular reference to the phenomenon of land consumption. The methodology follows the Cross-industry standard process for data mining (CRISP-DM) model, which is adapted to the study needs owing to its flexibility of use. The CRISP-DM is already used in the data mining field and describes the main phases of a project and their mutual relationship [43,44]. The classification methodology was tested with reference to three different configurations (called “scenarios”):

1. Scenario 1—binary classification distinguishing buildings from the residual areas;
2. Scenario 2—binary classification distinguishing consumed land and non-consumed land;
3. Scenario 3—identification and distinction of different consumed land classes from natural areas.

For each scenario, different sets of model parameters were tested in order to identify the most promising scenario and its most appropriate set of parameters. The optimal configuration was then used in the deployment phase for the classification of images in areas other than the training ones.

The processes were developed using PyTorch, an open-source machine learning library available for python programming language (<https://pytorch.org/>, accessed on 29 April 2022). The accuracy of the classifications produced by previously trained models was evaluated with the Semi-automatic Classification Plugin (SCP) for QGIS [45]. The methodology (Figure 3) is described in the following sections.

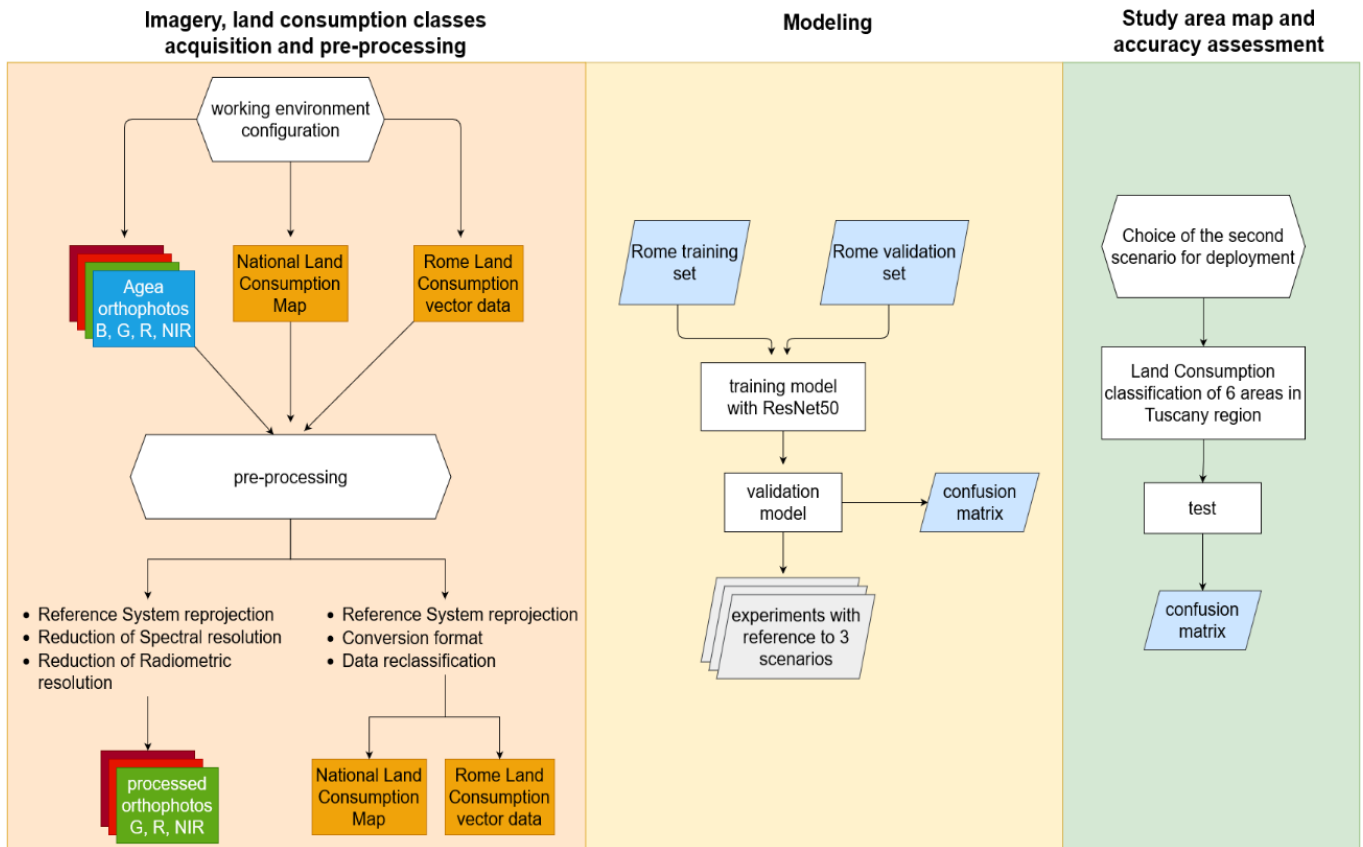


**Figure 3.** Study workflow.

### 2.3. Data Pre-Processing and Modeling

The training of the predictive model was carried out starting with two high-resolution images related to a portion of the municipality of Rome. The area was chosen because it is characterized by a fragmented landscape and a heterogeneous composition in terms of land cover, which is suitable for conducting land consumption studies. In detail, AGEA data relating to 2017 with a spatial resolution of 20 cm and four channels (red, green, blue, IR) were used ([https://www.agea.gov.it/portal/page/portal/AGEAPageGroup/HomeAGEA/Serviziutilita/Modulistica/Modulo\\_richiesta%20ortofoto](https://www.agea.gov.it/portal/page/portal/AGEAPageGroup/HomeAGEA/Serviziutilita/Modulistica/Modulo_richiesta%20ortofoto), accessed on 29 April 2022). The first orthophoto (a) of Figure 2 is used for the model training, while the second one (b) is used to verify the predictive capabilities of the model and then to validate it. The dataset was labeled using the vector version of the Land Consumption Map (LCM) produced and updated by ISPRA-SNPA. The vector data is available only for the territory of the municipality of Rome and is based on images with the same characteristics as the orthophotos used in this research [2]. The labeling process consisted of combining vector elements with the ground truth provided by the orthophotos, in order to achieve training and validation datasets.

#### 2.3.1. Pre-Processing

The input datasets were preprocessed before the land cover classification based on the DL approach:

1. The AGEA orthophotos (in raster format) were reprojected in the UTM WGS84 reference system and resampled to obtain square pixels. The spectral resolution was reduced to 3 bands: the blue region (500–520 nm) was removed since it is the least significant for artificial surfaces classification, although it led to a reduction in the information content. The radiometric resolution was also reduced: the 16 bit orthophotos were converted into 8 bit ones.
2. The LCM was reprojected in the UTM WGS84 reference system, subjected to topological verification, and converted to Geojson format. The map has a three-level classification system, which distinguishes different consumed land classes. The data was reclassified to be suitable for the analysis of the three scenarios (Table 1).

**Table 1.** LCM reclassification table with respect to the three scenarios. For the first scenario, the class of “buildings” was highlighted; in the second scenario the consumed land classes were separated from natural surfaces; and in the third one, the different consumed land classes were considered separately.

Class Name	LCM Code	Reclassification Code		
		Scenario 1	Scenario 2	Scenario 3
Buildings	111	1	1	1
Paved roads	112	0	1	2
Other non-built-up sealed areas	116	0	1	3
Unpaved roads	121	0	1	4
Construction sites and other clayey areas	122	0	1	5
Non-consumed land	2	0	0	0
Artificial waterbodies	201	0	0	0
Roundabouts and junctions	202	0	0	0
Unpaved greenhouses	203	0	0	0

### 2.3.2. Deep Residual Networks

A CNN is a neural network that is an algorithm with a hierarchical structure used to recognize patterns in data. It typically consists of three kinds of layers: convolutional layers, pooling layers, and fully-connected layers. Various CNN models are commonly used in remote sensing investigations such as U-Net [46], DenseNet [47], SegNet [48], and ResNet [49] and the latter model was chosen for the study. It was decided to use ResNet since its structure has shown good capabilities in similar applications and with a wide range of datasets [29,49,50]. ResNet (Residual Network) was first introduced in 2015 by He [51] for image recognition purposes and has had great success in remote sensing applications [49,52,53].

The ResNet model includes several variants which differ in number of neural network layers: ResNet-18, ResNet-34, ResNet-50, ResNet-101, and ResNet-152. These architectures were introduced to solve the vanishing gradient problem in order to improve the accuracy and performance of the model. To this end, ResNet uses a novel component in addition to the traditional ones, called residual block. The new block is a stack of layers that applies the skip connection technique: in other words, the output of a layer is used to feed a layer that is not directly adjacent. Considering the accuracy levels, the available times, and computational resources, ResNet-50 was implemented.

ResNet-50 (Figure 4) consists of 50 layers which include 48 convolutions, 1 max pooling, and 1 average pooling. A final full-connected layer and a softmax function complete the network. Like any ResNet architecture, it starts with a convolution and max-pooling layer using  $7 \times 7$  and  $3 \times 3$  kernel sizes, respectively. Afterward, the ResNet-50 proceeds with its 4 stages, which include 3 residual blocks for each [51].

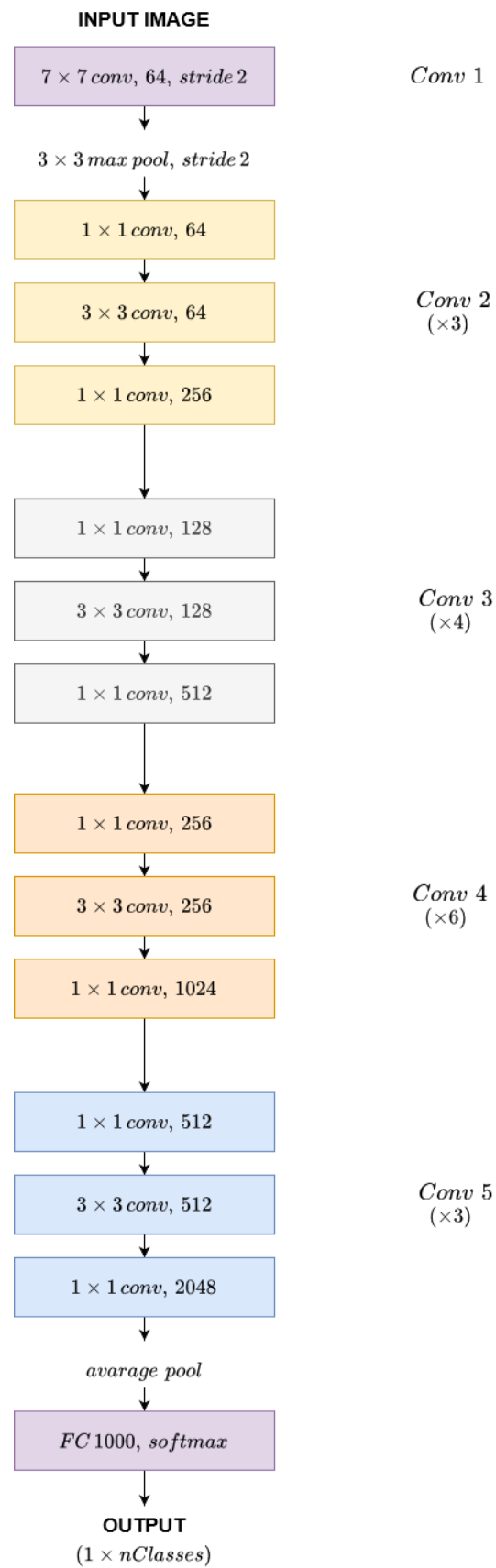


**Figure 4.** ResNet50 architecture.

### 2.3.3. Modeling

Modeling is the main phase of a DL experiment. The applied task can be categorized as semantic segmentation or pixel-by-pixel classification. The goal is labeling every pixel of an image with the corresponding semantic class using an automatic procedure. Convolutional neural networks (CNN) are well suited to gain test set labels. For this study, monotemporal input data was used to form a deep learning model, based on Resnet50 architecture [51].

The training phase was carried out considering 4 hyperparameters: chip size, chips per scene, batch size, and number of epochs. A total of 60 sets of values (called “experiments”) were defined, each corresponding to a different combination of hyperparameter values; the 60 experiments were applied to the 3 scenarios in order to evaluate which combination of scenario and experiment provides the best results. Hyperparameter tuning is crucial for the quality of the prediction and this depended on the data analyst assessments. Choices were based on computer performance and on “trial and error”. Each image was divided into chips (clippings of images) with dimensions ranging from  $50 \times 50$  to  $300 \times 300$  pixels, in relation to the extent of the image. Some of these chips were randomly extracted and used for model training: generally, we opted for a number of chips between 35 and 70 and a batch size smaller than 8. Randomization of image chips is advantageous as it ensures an independent distribution of samples and it is further justified in the case of study areas affected by urban sprawl. To identify the optimal hyperparameter values, several iterations were fitted; the model was trained using a random initialization of 5 epochs, up to the final model with 15 epochs. By increasing the number of epochs to 15, a constant trend was found for each scenario, which made it possible to compare them and identify the most promising one.

The result of the algorithm training was verified graphically by overlapping the produced maps, and through evaluation metrics reading. These metrics were calculated starting from the confusion matrix generated during the validation step.

The main indices computed are shown below:

$$\text{Precision} = \frac{(\text{True Positive})}{(\text{True Positive} + \text{False Positive})}, \quad (1)$$

$$\text{Recall} = \frac{(\text{True Positive})}{(\text{True Positive} + \text{False Negative})}, \quad (2)$$

$$\text{F1-score} = 2 \times \frac{\text{Recall} \times \text{Precision}}{\text{Recall} + \text{Precision}}, \quad (3)$$

### 2.4. Deployment and Accuracy Assessment

To verify the algorithm’s ability to identify consumed land and its effectiveness on areas other than training areas, the methodology was applied to 6 AGEA images relating to the Tuscan territory. The areas were chosen in order to test the effectiveness of the algorithm on territories with different degrees of consumed land. Tiles 2 and 3 have a similar presence of consumed land compared with the training areas, while natural areas prevail in tiles 4, 5, and 6, where much of the consumed land is made up of roads. In detail, reference was made to the scenario (and its corresponding set of hyperparameters) that showed the best results. For this application, the chosen scenario was tested on a higher number of epochs, specifically 30. The classifications obtained were then compared with the ISPRA LCM, which is only available in raster format for the study area. This data is a nationwide 10 m resolution raster with a three-level classification system capable of distinguishing different classes of reversible and permanent consumed land. The LCM is obtained starting from the classification of rapid-eye images, integrated with OpenStreetMap data for road mapping and improved and updated through photointerpretation. For a detailed description of the LCM specifications, see [6,17,54]. To compare it with the LCM, the classification was resampled to 10 m of resolution, associating each pixel with a percentage artificial density value. The artificial surface density raster was then reclassified into a binary raster, associating

the value 1 (consumed land) to the pixels with over 51% of the territory consumed, and 0 (not consumed land) to the others. These thresholds were chosen to make the two data comparable (in fact they are the same thresholds as the raster version of the LCM). Since the chosen approach uses a binary classification system (consumed land–non consumed land), the binary raster of the LCM was considered for the quantitative verification.

A confusion matrix was generated from the datasets comparison and the accuracy assessment was performed.

Overall accuracy: classification accuracy compared with ground truth:

$$\text{Overall Accuracy (\%)} = \frac{\text{number of correctly classified pixels}}{\text{total number of pixels}} \times 100 \quad (4)$$

User's accuracy: check how many pixels of a class  $i$  are correctly classified for the user:

$$\text{User's Accuracy (\%)} = \frac{\text{number of correctly classified pixels in class } i}{\text{number of pixels classified as class } i \text{ (total row)}} \times 100 \quad (5)$$

Producer's accuracy: check how many pixels of a class  $i$  are correctly classified for the producer:

$$\text{Producer's Accuracy (\%)} = \frac{\text{number of correctly classified pixels in class } i}{\text{number of known pixels in class } i \text{ (total column)}} \times 100 \quad (6)$$

Kappa coefficient: statistical index for assessing the degree of agreement between two assessments:

$$\text{Kappa coefficient} = \frac{\text{observed agreement} - \text{hypothetical probability}}{1 - \text{hypothetical probability}} \quad (7)$$

### 3. Results

#### 3.1. Modeling

This paragraph shows the results of testing the DL in consumed land mapping using different model parameters and different reference classes. For the training of the algorithm, 60 experiments (distinct configurations of the model parameters) were considered. Figures 5–7 show four representative results for each of the three scenarios.

The results obtained applying the 60 experiments to the three approaches were compared (Figures 5–7) in order to identify the most promising configuration. Scenario 2 shows the best results even by varying the number of epochs and was subjected to evaluation metrics analysis (Table 2) in order to identify the most reliable experiment. This analysis is referred to as a 30-epoch training.

#### 3.2. Deployment

The classification of the six orthophotos (Figure 8) relating to the study area was conducted with reference to experiment B1 of the second scenario. The results were analyzed in order to verify if the methodology allows the achievement of objectives two and three. In detail, two levels of analysis were conducted:

1. First, a visual comparison with orthophotos;
2. Then, calculating the accuracy with the SCP plug-in by comparing predictions with the binary version of the LCM (1 = consumed land, 0 = non-consumed land) (Table 3).

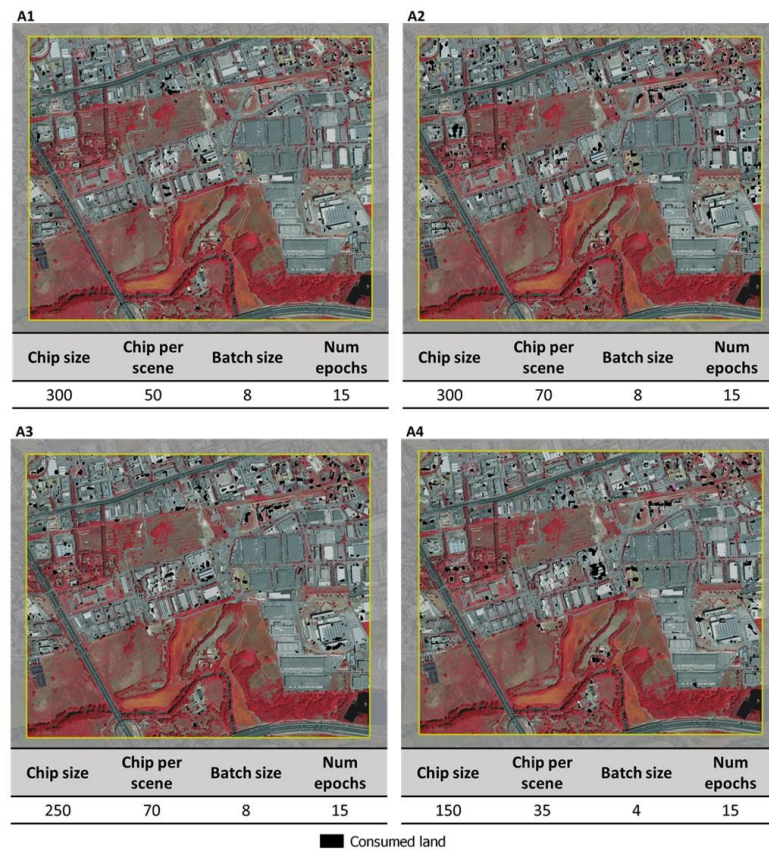


Figure 5. Classification examples relating to the first scenario, with reference to 4 distinct experiments.

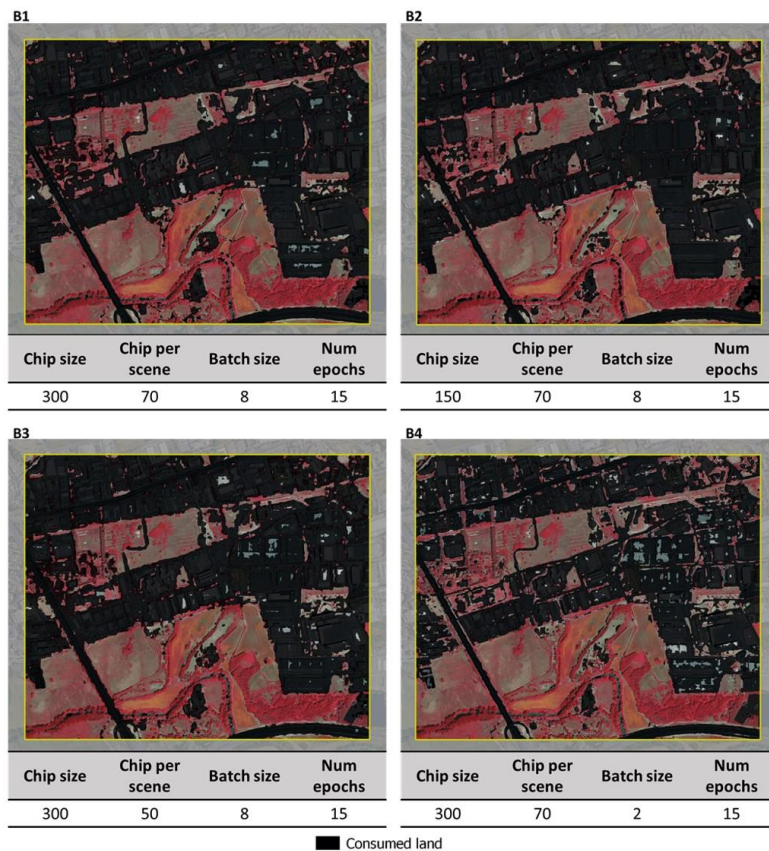


Figure 6. Classification examples relating to the second scenario, with reference to 4 distinct experiments.

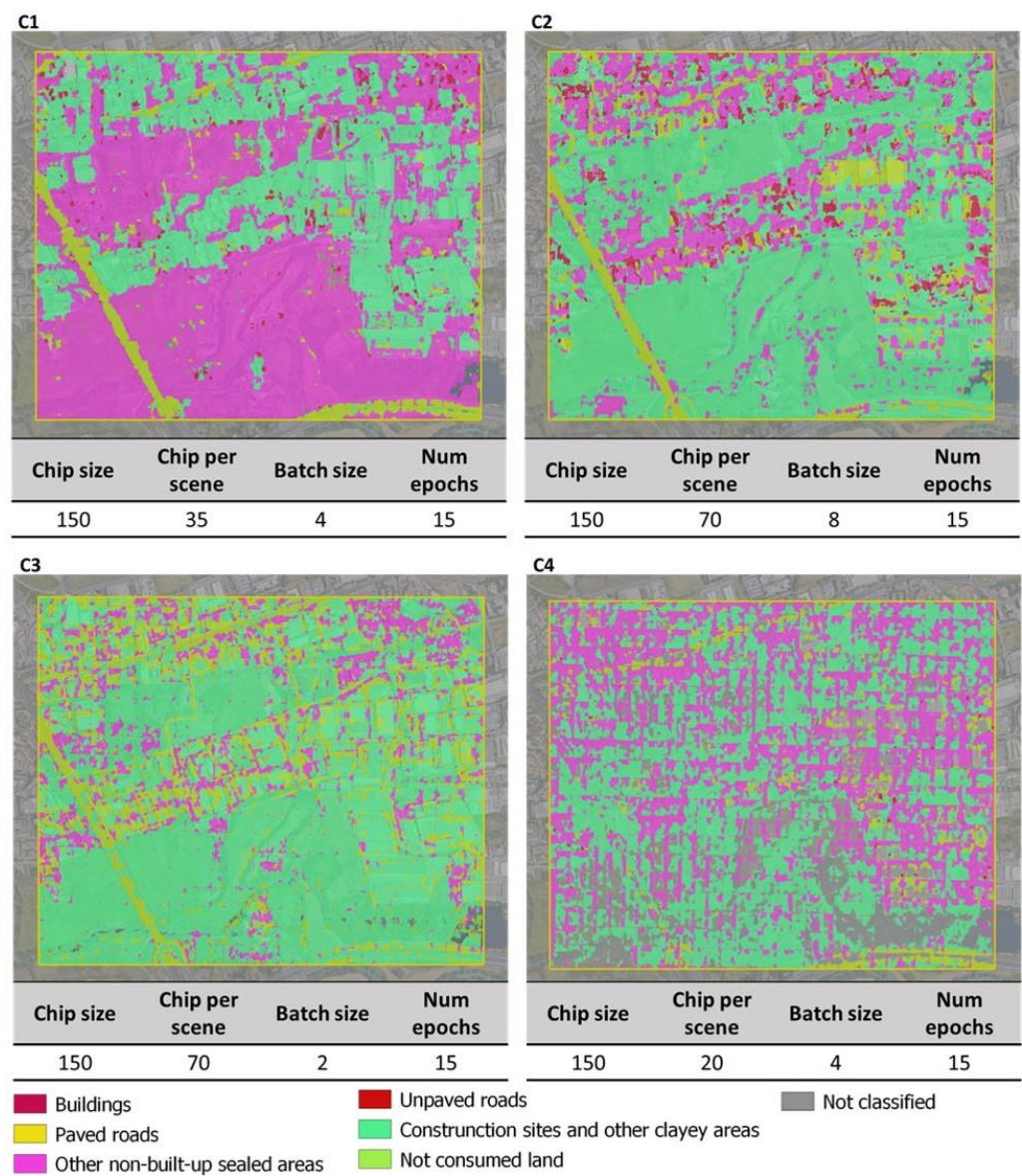


Figure 7. Classification examples relating to the third scenario, with reference to 4 distinct experiments.

Table 2. Scores of the four best experiments related to the second scenario. Class 0 identifies non-consumed land; class 1 identifies consumed land.

Accuracy	Experiment ID							
	B1		B2		B3		B4	
	Class 0	Class 1	Class 0	Class 1	Class 0	Class 1	Class 0	Class 1
Precision	0.931	0.890	0.926	0.863	0.876	0.852	0.881	0.936
Recall	0.897	0.825	0.872	0.822	0.869	0.763	0.944	0.759
F1-score	0.914	0.856	0.898	0.842	0.873	0.805	0.912	0.838

**Table 3.** Accuracy assessment by comparison with the LCM; 1 = consumed land, 0 = non-consumed land.

Tile 1 Kappa = 0.32					
Land Consumption Map					
		1	0	Tot. surface	Commission error
DL classification	1	11	8	19	41.55
	0	36	1075	1111	3.27
	Tot. surface	48	1083	1131	-
	Omission error	76.34	0.74	-	96.07
Tile 2 Kappa = 0.73					
Land Consumption Map					
		1	0	Tot. surface	Commission error
DL classification	1	200	32	232	13.70
	2	75	824	899	8.35
	Tot. surface	275	856	1131	-
	Omission error	27.30	3.71	-	90.56
Tile 3 Kappa = 0.61					
Land Consumption Map					
		1	0	Tot. surface	Commission error
DL classification	1	95	37	133	28.13
	0	61	941	1002	6.09
	Tot. surface	156	978	1134	-
	Omission error	39.01	3.82	-	91.33
Tile 4 Kappa = 0.38					
Land Consumption Map					
		1	0	Tot. surface	Commission error
DL classification	1	4	2	7	34.49
	0	11	1120	1131	0.95
	Tot. surface	15	1123	1138	-
	Omission error	71.12	0.20	-	98.86
Tile 5 Kappa = 0.37					

Table 3. Cont.

Land Consumption Map					
DL classification		1	0	Tot. surface	Commission error
	1	6	6	13	51.03
	0	14	1168	1183	1.21
	Tot. surface	21	1175	1195	-
Omission error	69.74	0.55	-	98.26	

Tile 6 Kappa = 0.29

Land Consumption Map					
DL classification		1	0	Tot. surface	Commission error
	1	6	3	10	35.65
	0	25	1100	1125	2.25
	Tot. surface	32	1103	1135	-
Omission error	80.32	0.31	-	97.46	

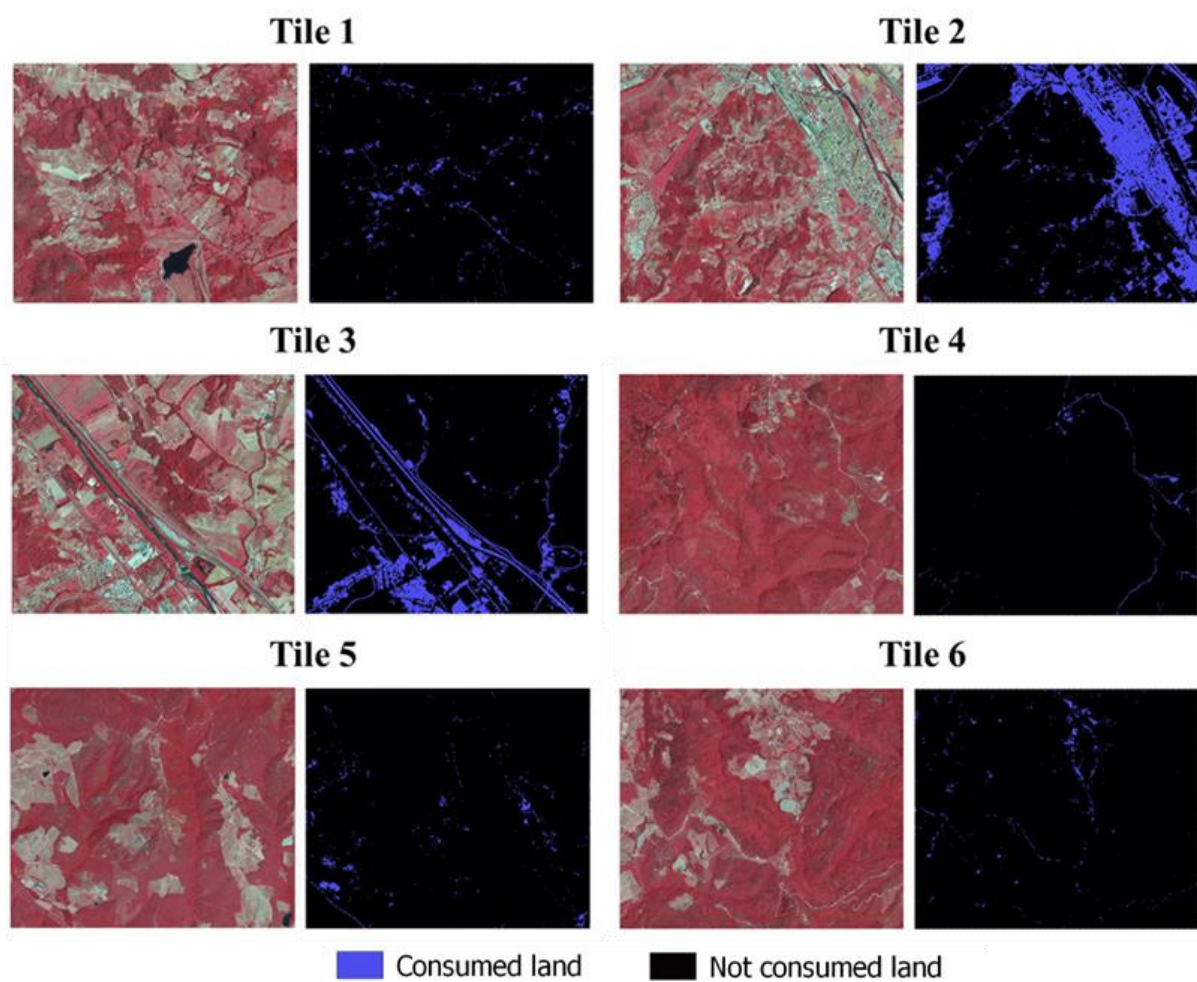


Figure 8. Classification results of the 6 study areas relating to B1 configuration.

#### 4. Discussion

This research represents the first attempt to integrate DL techniques in the process of updating the LCM produced by ISPRA at the national scale and with high frequency. In this sense, the mapping of the consumed land is a preliminary step for the definition of support tools for the photointerpretation of land consumption in the future for the automation of the updating process, limiting the intervention of the operator as much as possible.

The first objective of the research concerned the verification of the applicability of the DL for the mapping of the consumed land, with reference to the classification of very high-resolution images for the Italian territory. Three different scenarios were illustrated: two binary classifications and a multi-category one. The analysis of the three methodologies highlights the second one (binary classification of consumed and non-consumed land) as the most accurate. As a matter of fact, the strategy of merging all the artificial surfaces into a single class produced good results. Slight variations between experiments are dictated by chip and batch size. Decreasing the batch number and using smaller chips, more precision was found in road boundaries and omission errors were reduced.

The second objective of the research concerned the possibility of automatically producing thematic maps with the aim of improving accuracy and reducing costs and time. Overall, the methodology allows to obtain consumed land classifications in a short time with good results especially on artificial areas, while the classification of shaded areas and reversible consumed land is still to be perfected. The first results are promising and show a good ability of the data to identify even small consumed areas. In this sense, we intend to perfect the methodology to produce diachronic classifications of the consumed land to obtain layers of potential changes, suitable in the first instance to support and increase the speed of the photointerpretation process in the most dynamic areas. In detail, the semantic segmentation algorithm was trained and deployed on a personal computer (spec- 12 GB RAM, Intel core i5-6200U CPU @ 2.40 GHz), which took roughly 50 min to complete the most efficient experiment running on CPU. Considering the available computing resources, the entire process required relatively short processing times. The speed of processing confirms the promising capabilities of the methodology in land monitoring. In the accuracy assessment, the classifications were compared with the LCM, which is the national benchmark for this theme. The methodology shows good results in the recognition of the built areas (Figure 9a), even the smallest ones. Looking at the results of Table 3 it is important to take into account that in some cases the algorithm correctly identifies consumed land which is not detected by the LCM (Figure 9d). In other cases, false omission and commission errors on properly mapped land consumed areas are related to the non-alignment caused by the different characteristics of the two data (Figure 9e). In detail, the best results are obtained for tiles 2 and 3 ( $Kappa = 0.73$  and  $0.61$ , respectively) (Table 3), which are characterized by the highest presence of built-up areas, while the lowest values are related to tiles 4, 5, and 6, which are characterized by a low density of buildings and consumed land is primarily determined by the presence of roads. Systematic errors that affect accuracy are due to the still experimental nature of the methodology. Commission errors are mainly located in tiles 2 and 3 and they correspond to a river mapped as consumed land. The error is due to the lack of training areas for this land cover class. Other minor commissions concern uncultivated agricultural areas in the reference period. The methodology shows higher accuracy in built-up areas, while in sparsely urbanized areas the accuracy is strongly affected by the errors associated with the mapping of the roads. In this regard, comparing the results of the accuracy assessment with the LCM at the third classification level helps to analyze the consumed classes that show more classification errors. In detail, omission errors mainly affect the road network, which is not mapped correctly in the presence of buildings or rows of trees near the roads (Figure 9b). Portions of road not covered by shadows or obstacles are correctly mapped. It should be noted that the LCM uses the OpenStreetMap database for mapping roads, which has been updated by photointerpretation; therefore, it is characterized by high accuracy even for hidden roads, which are difficult to map only through spectral information. Other omission errors mainly refer to areas

mapped by the LCM as reversible consumed land. This category includes unpaved roads, sports fields, and other areas where soil has been removed (Figure 9c), many of which are partially renaturalized. The complexity in distinguishing bare soil from sealed surfaces is underlined in several experiences [55,56]. In this regard, a bibliographic analysis offers the possibility to introduce and use hyperspectral data [39,57,58], SAR data [59], or consider multitemporal data [60] to improve the recognition of urban or industrial areas and bare soil and to verify their evolution during the year, evaluating the appearance of vegetation or the occurrence of changes.

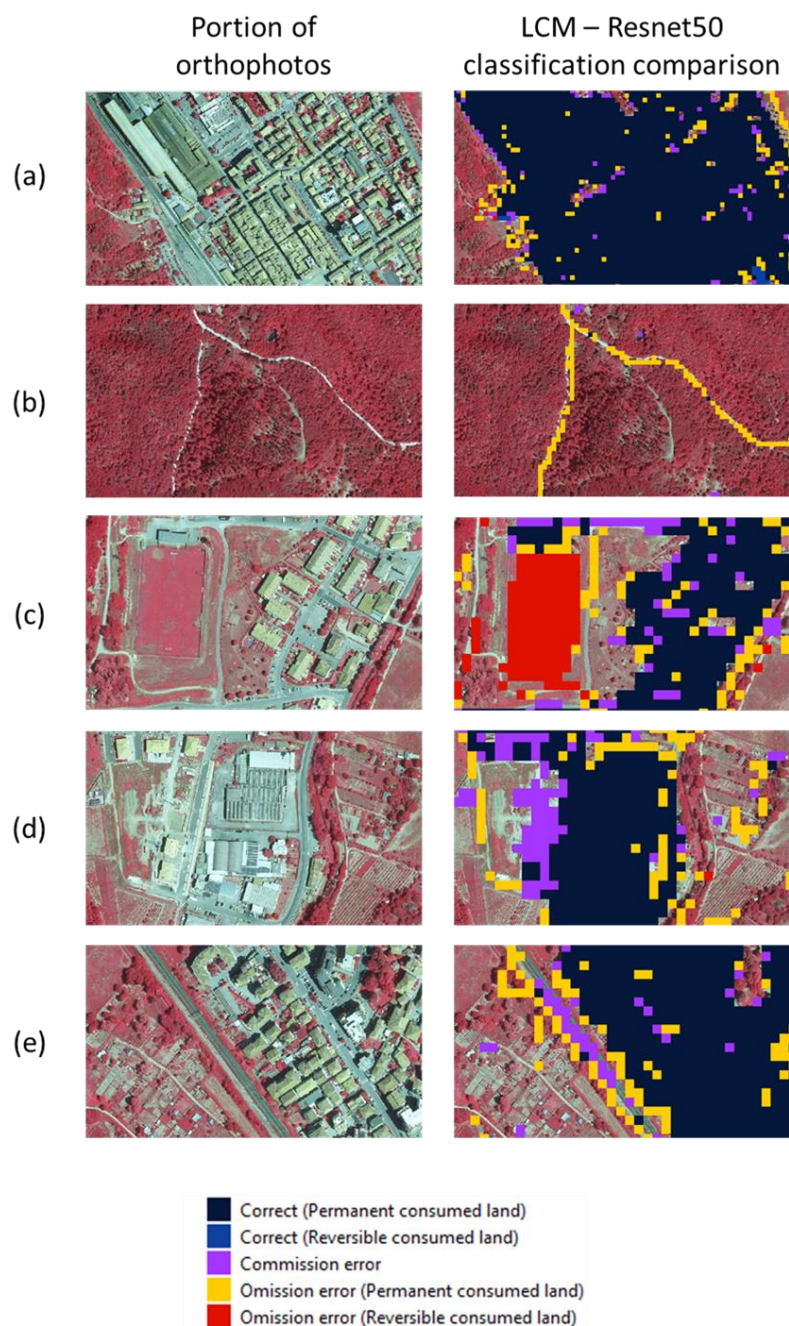


**Figure 9.** Comparison of the classification results with LCM: (a) Example of an excellent recognition of built-up areas; (b) omission error of a secondary road in a forest area; (c) omission error referred to as a sports field mapped by the LCM as reversible consumed land; (d) example of the DL algorithm correctly mapping an area that LCM does not identify as consumed land; and (e) errors related to the different resolutions of the two considered data.

The third objective of the research aims to demonstrate the strategic importance of using artificial intelligence for the land consumption mapping. If a first important objective concerns refinement in the identification of reversible consumed land, a further significant step forward will be linked to its use for the detection of land consumption. The study was developed together with other ISPRA activities [1,6,17] for the creation of tools that can facilitate and expedite land consumption monitoring operations. In this sense, the methodology is already a useful tool at present, allowing the rapid production of support layers for photointerpretation and it is useful for identifying the areas of potential change. Compared with other tools already developed by ISPRA [17], the higher spatial resolution of these products makes them particularly suitable for detecting changes in the peri-urban area, where the greater density of small changes is generally concentrated. However, future developments are possible with the methodology. Compared with the traditional algorithms of ML (decision trees, random forest, K-nearest neighbor, etc.), the DL is an adaptive system that is self-regulated according to the input data. The purpose of the DL is to find the most complex and hidden relationships between data, with the aim to reduce the human intervention as much as possible. Furthermore, ANNs allow to analyze raw data without heavy pre-processing and they can recognize distorted and rotated elements. The current state-of-the-art of the DL for land monitoring applications allows achieving good results only by using very high-resolution images, which are not free of charge. An interesting future methodology development could concern the experimentation of the most modern architectures of ANNs with multispectral high-resolution images. For example, the use of Sentinel images of the Copernicus Program would allow the availability of free, multitemporal, and multispectral data, with important advantages from the point of view of classification. The use of multispectral data allows researchers to better distinguish the surfaces based on their spectral characteristics, while analyzing the temporal variation of the land cover surfaces would allow evaluation of their permanence. This, together with the choice of appropriate parameters of the neural network, are potential approaches aimed at improving accuracy. Given the encouraging results in the medium–high-density urban environment, DL algorithms could represent a turning point for land consumption monitoring in peri-urban areas, which are extremely dynamic areas that need special attention and timely interventions.

## 5. Conclusions

This study introduces a spectral–spatial DL-based model for consumed land mapping. The proposed method experiments with a CNN network called ResNet50 on a reference dataset of high spatial resolution aerial images, considering three scenarios. The performances achieved reveal its promising capabilities in land monitoring if optimal parameters and scenes are used for model training: as a matter of fact, the analysis of the three scenarios shows that the training scene choice has a serious impact on classification accuracy.

Regarding objective two, the comparison with the LCM shows high congruence in permanent consumed land mapping and, in some cases, the CNN model was proven to be more effective than LCM. On the other hand, mapping reversible consumed land is more challenging, due to the need to consider land use characteristics in addition to land cover. In this sense, it is possible to try to improve the accuracy of the methodology by focusing on a more accurate choice of training datasets and integrating different types of data (such as multispectral images or multitemporal datasets) and on the optimization of the parameters. The reliability of the model is strongly influenced by the choice of input data and parameters and is therefore not suitable for application in a vast and heterogeneous territory; however, the results show high reliability in medium–high-density areas. It follows that the methodology would be useful to support land consumption monitoring in peri-urban areas, which are among the areas most affected by the phenomenon [2].

Following the guidelines of the European Commission, in order to achieve the goal “no net land take” by 2050 [61], it is necessary to map and monitor land consumption to avoid its negative consequences, such as loss of high-quality agricultural land, the effects

on climate change, biodiversity loss, increased risk of flooding, etc. Overall, regarding the third theme, owing to the high accuracy obtained with the proposed model, improvements in permanent consumed land detection can be achieved. If properly developed, this methodology could provide a valuable aid in change detection applications. Therefore, deep learning techniques could contribute to updating the National Land Consumption Map and to a more efficient production of environmental indicators. Deep learning is a rapidly expanding technology; however, it is still not widespread enough for land monitoring and land consumption mapping, although it would lead to concrete progress in these fields. It is therefore essential to raise research awareness even in the non-informatics field, with the aim to acquire enough knowledge and practice to exploit the most sophisticated cutting-edge techniques.

**Author Contributions:** Conceptualization, G.C., L.C. and M.M. (Michele Munafò); methodology, G.C. and L.C.; software, G.C., P.D.F. and L.C.; validation, G.C. and P.D.F.; formal analysis, G.C., P.D.F. and L.C.; investigation, G.C. and L.C.; resources, M.M. (Michele Munafò) and M.M. (Marco Marchetti); data curation, G.C., P.D.F. and L.C.; writing—original draft preparation, G.C. and P.D.F.; visualization, G.C. and P.D.F.; supervision, L.C., M.M. (Michele Munafò) and M.M. (Marco Marchetti); and funding acquisition, M.M. (Marco Marchetti). All authors have read and agreed to the published version of the manuscript.

**Funding:** This research was funded by the University of Molise.

**Institutional Review Board Statement:** Not applicable.

**Informed Consent Statement:** Not applicable.

**Data Availability Statement:** The data are not publicly available because they are part of ongoing research.

**Conflicts of Interest:** The authors declare no conflict of interest.

## References

- De Fioravante, P.; Luti, T.; Cavalli, A.; Giuliani, C.; Dichicco, P.; Marchetti, M.; Chirici, G.; Congedo, L.; Munafò, M. Multispectral Sentinel-2 and Sar Sentinel-1 Integration for Automatic Land Cover Classification. *Land* **2021**, *10*, 611. [[CrossRef](#)]
- Munafò, M. *Consumo Di Suolo, Dinamiche Territoriali e Servizi Ecosistemici*; Edizione 2021; ISPRA, SNPA: Rome, Italy, 2021; ISBN 9788844810597.
- Chirici, G.; Giannetti, F.; Mazza, E.; Francini, S.; Travaglini, D.; Pegna, R.; White, J.C. Monitoring Clearcutting and Subsequent Rapid Recovery in Mediterranean Coppice Forests with Landsat Time Series. *Ann. For. Sci.* **2020**, *77*, 1–14. [[CrossRef](#)]
- Marchetti, M.; Vizzarri, M.; Sallustio, L. Towards Countryside Revival: Reducing Impacts of Urban Expansion on Land Benefits. In *Agrourbanism*; Springer: Berlin/Heidelberg, Germany, 2019; pp. 207–222.
- Costanza, R.; d’Arge, R.; de Groot, R.; Farber, S.; Grasso, M.; Hannon, B.; Limburg, K.; Naeem, S.; O’neill, R.V.; Paruelo, J. The Value of the World’s Ecosystem Services and Natural Capital. *Nature* **1997**, *387*, 253–260. [[CrossRef](#)]
- Strollo, A.; Smiraglia, D.; Bruno, R.; Assennato, F.; Congedo, L.; de Fioravante, P.; Giuliani, C.; Marinosci, I.; Riitano, N.; Munafò, M. Land Consumption in Italy. *J. Maps* **2020**, *16*, 113–123. [[CrossRef](#)]
- Shukla, P.R.; Skeg, J.; Buendia, E.C.; Masson-Delmotte, V.; Pörtner, H.-O.; Roberts, D.C.; Zhai, P.; Slade, R.; Connors, S.; van Diemen, S. *Climate Change and Land: An IPCC Special Report on Climate Change, Desertification, Land Degradation, Sustainable Land Management, Food Security, and Greenhouse Gas Fluxes in Terrestrial Ecosystems*; Intergovernmental Panel on Climate Change: Geneva, Switzerland, 2019.
- Dewan, A.M.; Yamaguchi, Y. Land Use and Land Cover Change in Greater Dhaka, Bangladesh: Using Remote Sensing to Promote Sustainable Urbanization. *Appl. Geogr.* **2009**, *29*, 390–401. [[CrossRef](#)]
- Lal, R. Restoring Soil Quality to Mitigate Soil Degradation. *Sustainability* **2015**, *7*, 5875–5895. [[CrossRef](#)]
- Oldeman, L.R.; Hakkeling, R.T.A.; Sombroek, W.G. *World Map of the Status of Human-Induced Soil Degradation: An Explanatory Note*; International Soil Reference and Information Centre: Wageningen, The Netherlands, 1990; ISBN 9066720425.
- Cowie, A.L.; Orr, B.J.; Castillo Sanchez, V.M.; Chasek, P.; Crossman, N.D.; Erlewein, A.; Louwagie, G.; Maron, M.; Metternicht, G.I.; Minelli, S.; et al. Land in Balance: The Scientific Conceptual Framework for Land Degradation Neutrality. *Environ. Sci. Policy* **2018**, *79*, 25–35. [[CrossRef](#)]
- Attri, P.; Chaudhry, S.; Sharma, S. Remote Sensing & GIS Based Approaches for LULC Change Detection—A Review. *Int. J. Curr. Eng. Technol.* **2015**, *5*, 3126–3137.
- Shalaby, A.; Tateishi, R. Remote Sensing and GIS for Mapping and Monitoring Land Cover and Land-Use Changes in the Northwestern Coastal Zone of Egypt. *Appl. Geogr.* **2007**, *27*, 28–41. [[CrossRef](#)]

14. Rogan, J.; Chen, D.M. Remote Sensing Technology for Mapping and Monitoring Land-Cover and Land-Use Change. *Prog. Plan.* **2004**, *61*, 301–325. [[CrossRef](#)]
15. Winkler, K.; Fuchs, R.; Rounsevell, M.; Herold, M. Global Land Use Changes Are Four Times Greater than Previously Estimated. *Nat. Commun.* **2021**, *12*, 2501. [[CrossRef](#)] [[PubMed](#)]
16. Solórzano, J.V.; Mas, J.F.; Gao, Y.; Gallardo-Cruz, J.A. Land Use Land Cover Classification with U-Net: Advantages of Combining Sentinel-1 and Sentinel-2 Imagery. *Remote Sens.* **2021**, *13*, 3600. [[CrossRef](#)]
17. Luti, T.; de Fioravante, P.; Marinosci, I.; Strollo, A.; Riitano, N.; Falanga, V.; Mariani, L.; Congedo, L.; Munafò, M. Land Consumption Monitoring with Sar Data and Multispectral Indices. *Remote Sens.* **2021**, *13*, 1586. [[CrossRef](#)]
18. Munafò, M. *Consumo Di Suolo, Dinamiche Territoriali e Servizi Ecosistemici*; ISPRA, SNPA: Rome, Italy, 2019.
19. Gandomi, A.; Haider, M. Beyond the Hype: Big Data Concepts, Methods, and Analytics. *Int. J. Inf. Manag.* **2015**, *35*, 137–144. [[CrossRef](#)]
20. Audebert, N.; Saux, B.L.; Lefèvre, S. Semantic Segmentation of Earth Observation Data Using Multimodal and Multi-Scale Deep Networks. In Proceedings of the Asian Conference on Computer Vision, Taipei, Taiwan, 20–24 November 2016; pp. 180–196.
21. Soille, P.; Burger, A.; de Marchi, D.; Kempeneers, P.; Rodriguez, D.; Syrris, V.; Vasilev, V. A Versatile Data-Intensive Computing Platform for Information Retrieval from Big Geospatial Data. *Future Gener. Comput. Syst.* **2018**, *81*, 30–40. [[CrossRef](#)]
22. Gibert, K.; Horsburgh, J.S.; Athanasiadis, I.N.; Holmes, G. Environmental Data Science. *Environ. Model. Softw.* **2018**, *106*, 4–12. [[CrossRef](#)]
23. Hoerer, T.; Kuenzer, C. Object Detection and Image Segmentation with Deep Learning on Earth Observation Data: A Review-Part I: Evolution and Recent Trends. *Remote Sens.* **2020**, *12*, 1667. [[CrossRef](#)]
24. Barash, Y.; Guralnik, G.; Tau, N.; Soffer, S.; Levy, T.; Shimon, O.; Zimlichman, E.; Konen, E.; Klang, E. Comparison of Deep Learning Models for Natural Language Processing-Based Classification of Non-English Head CT Reports. *Neuroradiology* **2020**, *62*, 1247–1256. [[CrossRef](#)] [[PubMed](#)]
25. Affonso, C.; Rossi, A.L.D.; Vieira, F.H.A.; de Carvalho, A.C.P.; de Carvalho, L.F. Deep Learning for Biological Image Classification. *Expert Syst. Appl.* **2017**, *85*, 114–122. [[CrossRef](#)]
26. Debella-Gilo, M.; Gjertsen, A.K. Mapping Seasonal Agricultural Land Use Types Using Deep Learning on Sentinel-2 Image Time Series. *Remote Sens.* **2021**, *13*, 289. [[CrossRef](#)]
27. Makantasis, K.; Karantzalos, K.; Doulamis, A.; Doulamis, N. Deep Supervised Learning for Hyperspectral Data Classification through Convolutional Neural Networks. In Proceedings of the International Geoscience and Remote Sensing Symposium (IGARSS), Milan, Italy, 26–31 July 2015; Volume 2015, pp. 4959–4962.
28. Zhang, X.; Han, L.; Han, L.; Zhu, L. How Well Do Deep Learning-Based Methods for Land Cover Classification and Object Detection Perform on High Resolution Remote Sensing Imagery? *Remote Sens.* **2020**, *12*, 417. [[CrossRef](#)]
29. Li, Y.; Zhang, H.; Xue, X.; Jiang, Y.; Shen, Q. Deep Learning for Remote Sensing Image Classification: A Survey. *Wiley Interdiscip. Rev. Data Min. Knowl. Discov.* **2018**, *8*, e1264. [[CrossRef](#)]
30. LeCun, Y.; Bottou, L.; Bengio, Y.; Haffner, P. Gradient-Based Learning Applied to Document Recognition. *Proc. IEEE* **1998**, *86*, 2278–2324. [[CrossRef](#)]
31. Raschka, S.; Patterson, J.; Nolet, C. Machine Learning in Python: Main Developments and Technology Trends in Data Science, Machine Learning, and Artificial Intelligence. *Information* **2020**, *11*, 193. [[CrossRef](#)]
32. Jamali, A.; Mahdianpari, M.; Brisco, B.; Granger, J.; Mohammadimanesh, F.; Salehi, B. Comparing Solo versus Ensemble Convolutional Neural Networks for Wetland Classification Using Multi-Spectral Satellite Imagery. *Remote Sens.* **2021**, *13*, 2046. [[CrossRef](#)]
33. DeLancey, E.R.; Simms, J.F.; Mahdianpari, M.; Brisco, B.; Mahoney, C.; Kariyeva, J. Comparing Deep Learning and Shallow Learning for Large-Scale Wetland Classification in Alberta, Canada. *Remote Sens.* **2020**, *12*, 2. [[CrossRef](#)]
34. Arndt, J.; Lunga, D. Large-Scale Classification of Urban Structural Units from Remote Sensing Imagery. *IEEE J. Sel. Top Appl. Earth Obs. Remote Sens.* **2021**, *14*, 2634–2648. [[CrossRef](#)]
35. Reda, K.; Kedzierski, M. Detection, Classification and Boundary Regularization of Buildings in Satellite Imagery Using Faster Edge Region Convolutional Neural Networks. *Remote Sens.* **2020**, *12*, 2240. [[CrossRef](#)]
36. Liu, C.; Zeng, D.; Wu, H.; Wang, Y.; Jia, S.; Xin, L. Urban Land Cover Classification of High-Resolution Aerial Imagery Using a Relation-Enhanced Multiscale Convolutional Network. *Remote Sens.* **2020**, *12*, 311. [[CrossRef](#)]
37. El Mendili, L.; Puissant, A.; Chougrad, M.; Sebari, I. Towards a Multi-Temporal Deep Learning Approach for Mapping Urban Fabric Using Sentinel 2 Images. *Remote Sens.* **2020**, *12*, 423. [[CrossRef](#)]
38. Schmitt, M.; Wu, Y.L. Remote Sensing Image Classification with the SEN12MS Dataset. In Proceedings of the ISPRS Annals of the Photogrammetry, Remote Sensing and Spatial Information Sciences, Göttingen, Germany, 17 June 2021; Volume 5, pp. 101–106.
39. Kumar, V.; Singh, R.S.; Dua, Y. Morphologically Dilated Convolutional Neural Network for Hyperspectral Image Classification. *Signal Process. Image Commun.* **2022**, *101*, 116549. [[CrossRef](#)]
40. Saralioglu, E.; Gungor, O. Semantic Segmentation of Land Cover from High Resolution Multispectral Satellite Images by Spectral-Spatial Convolutional Neural Network. *Geocarto Int.* **2022**, *37*, 657–677. [[CrossRef](#)]
41. Scherer, D.; Müller, A.; Behnke, S. Evaluation of Pooling Operations in Convolutional Architectures for Object Recognition. In Proceedings of the International Conference on Artificial Neural Networks, Thessaloniki, Greece, 15–18 September 2010; pp. 92–101.

42. Marchetti, M.; Bertani, R.; Corona, P.; Valentini, R. Cambiamenti Di Copertura Forestale e Dell'uso Del Suolo Nell'inventario Dell'uso Delle Terre in Italia. *For. J. Silvic. For. Ecol.* **2012**, *9*, 170.
43. Martinez-Plumed, F.; Contreras-Ochando, L.; Ferri, C.; Hernandez-Orallo, J.; Kull, M.; Lachiche, N.; Ramirez-Quintana, M.J.; Flach, P. CRISP-DM Twenty Years Later: From Data Mining Processes to Data Science Trajectories. *IEEE Trans. Knowl. Data Eng.* **2021**, *33*, 3048–3061. [[CrossRef](#)]
44. Wirth, R.; Hipp, J. CRISP-DM: Towards a Standard Process Model for Data Mining. In Proceedings of the 4th International Conference on the Practical Applications of Knowledge Discovery and Data Mining, Manchester, UK, 11–13 April 2000; Volume 1, pp. 29–40.
45. Congedo, L. Semi-Automatic Classification Plugin: A Python Tool for the Download and Processing of Remote Sensing Images in QGIS. *J. Open Source Softw.* **2021**, *6*, 3172. [[CrossRef](#)]
46. Wang, S.; Chen, W.; Xie, S.M.; Azzari, G.; Lobell, D.B. Weakly Supervised Deep Learning for Segmentation of Remote Sensing Imagery. *Remote Sens.* **2020**, *12*, 207. [[CrossRef](#)]
47. Cai, H.; Chen, T.; Niu, R.; Plaza, A. Landslide Detection Using Densely Connected Convolutional Networks and Environmental Conditions. *IEEE J. Sel. Top. Appl. Earth Obs. Remote Sens.* **2021**, *14*, 5235–5247. [[CrossRef](#)]
48. Dong, Y.; Li, F.; Hong, W.; Zhou, X.; Ren, H. Land Cover Semantic Segmentation of Port Area with High Resolution SAR Images Based on SegNet. In Proceedings of the 2021 SAR in Big Data Era, BIGSAR DATA 2021—Proceedings, Nanjing, China, 22–24 September 2021.
49. Tong, X.Y.; Xia, G.S.; Lu, Q.; Shen, H.; Li, S.; You, S.; Zhang, L. Land-Cover Classification with High-Resolution Remote Sensing Images Using Transferable Deep Models. *Remote Sens. Environ.* **2020**, *237*, 111322. [[CrossRef](#)]
50. Qiu, C.; Mou, L.; Schmitt, M.; Zhu, X.X. Local Climate Zone-Based Urban Land Cover Classification from Multi-Seasonal Sentinel-2 Images with a Recurrent Residual Network. *ISPRS J. Photogramm. Remote Sens.* **2019**, *154*, 151–162. [[CrossRef](#)]
51. He, K.; Zhang, X.; Ren, S.; Sun, J. Deep Residual Learning for Image Recognition. *arXiv* **2015**, arXiv:1512.03385.
52. Tao, C.S.; Chen, S.W.; Xiao, S.P. Comparison Study of Multitemporal PolSAR Classification Using Convolutional Neural Networks. In Proceedings of the International Geoscience and Remote Sensing Symposium (IGARSS), Waikoloa, HI, USA, 26 September–2 October 2020; pp. 204–207.
53. Lobry, S.; Marcos, D.; Murray, J.; Tuia, D. RSVQA: Visual Question Answering for Remote Sensing Data. *IEEE Trans. Geosci. Remote Sens.* **2020**, *58*, 8555–8566. [[CrossRef](#)]
54. Munafò, M. *Consumo Di Suolo, Dinamiche Territoriali e Servizi Ecosistemici*; Edizione 2022; ISPRA, SNPA: Rome, Italy, 2022; ISBN 9788844811242.
55. Gao, H.; Guo, J.; Guo, P.; Chen, X. Classification of Very-high-spatial-resolution Aerial Images Based on Multiscale Features with Limited Semantic Information. *Remote Sens.* **2021**, *13*, 364. [[CrossRef](#)]
56. Luo, X.; Tong, X.; Hu, Z.; Wu, G. Improving Urban Land Cover/Use Mapping by Integrating a Hybrid Convolutional Neural Network and an Automatic Training Sample Expanding Strategy. *Remote Sens.* **2020**, *12*, 2292. [[CrossRef](#)]
57. Li, C.; Hang, R.; Rasti, B. EMFNet: Enhanced Multisource Fusion Network for Land Cover Classification. *IEEE J. Sel. Top. Appl. Earth Obs. Remote Sens.* **2021**, *14*, 4381–4389. [[CrossRef](#)]
58. Pande, S.; Banerjee, B. Adaptive Hybrid Attention Network for Hyperspectral Image Classification. *Pattern Recognit. Lett.* **2021**, *144*, 6–12. [[CrossRef](#)]
59. Avolio, C.; Tricomi, A.; Mammone, C.; Zavagli, M.; Costantini, M. A Deep Learning Architecture for Heterogeneous and Irregularly Sampled Remote Sensing Time Series. In Proceedings of the IGARSS 2019—2019 IEEE International Geoscience and Remote Sensing Symposium, Yokohama, Japan, 28 July–2 August 2019; pp. 9807–9810.
60. Qian, M.; Sun, S.; Li, X. Multimodal Data and Multiscale Kernel-Based Multistream Cnn for Fine Classification of a Complex Surface-Mined Area. *Remote Sens.* **2021**, *13*, 5052. [[CrossRef](#)]
61. European Commission. Directorate-General for the Environment. In *FUTURE BRIEF: No Net Land Take by 2050?* Directorate-General for Agriculture and Rural Development: Brussels, Belgium, 2016; ISBN 9789279457395.